Journal of Physics: Conference Series

PAPER • **OPEN ACCESS**

Scheduling optimization model for integrated energy systems considering conditional value-at-risk

To cite this article: Q Peng *et al* 2020 *J. Phys.: Conf. Ser.* **1585** 012043

View the article online for updates and enhancements.

You may also like

- Solving portfolio selection problems with minimum transaction lots based on conditional-value-at-risk
E.P. Setiawan and D. Rosadi
- Using measurable dosimetric quantities to characterize the inter-structural tradeoff in inverse planning
Hongcheng Liu, Peng Dong and Lei Xing
- Portfolio Purchasing Decision for Mobile Power Equipment of B2C E-Commerce Export Retailer Based on CVaR
Wan Yanchun and Chen Qiucen

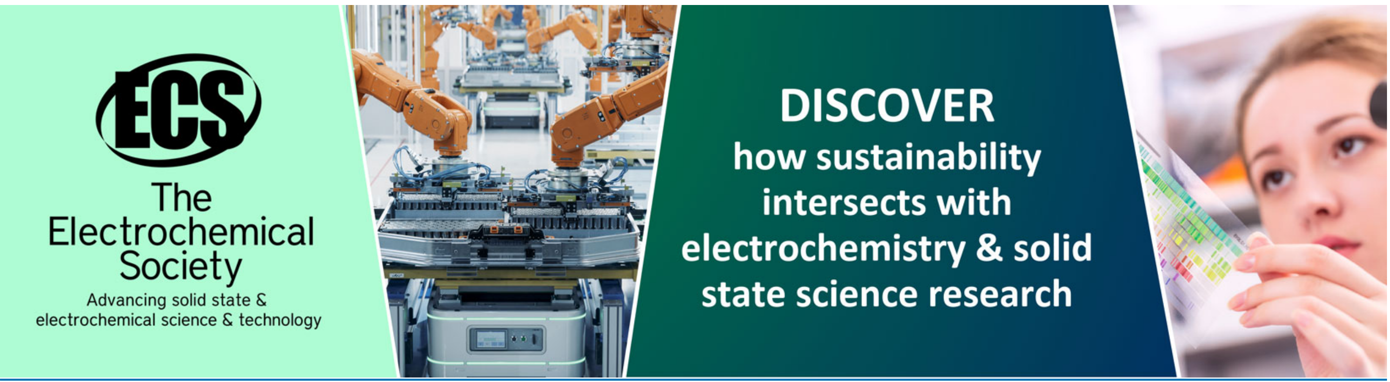

This content was downloaded from IP address 18.117.142.248 on 06/05/2024 at 13:13

Scheduling optimization model for integrated energy systems considering conditional value-at-risk

Q Peng[1], X L Wang[1], S X Qi[1], Z D Wang[2], S Yan[3] and Y T Chen[1]

[1]Xian Jiaotong University, Xi'an, Shaanxi, 710049, P.R. China
[2]State Grid Economic and Technological Research Institute Co., LTD., Beijing, 102209, P.R. China
[3]State Grid Corporation of China, Beijing, 100031, P.R. China

pengqiaopq@stu.xjtu.edu.cn

Abstract. The integrated energy system (IES) promotes the integration of renewable energy and improves energy efficiency, but it also brings uncertainty to the system. The uncertainty of the output of renewable energy may lead to imbalance of supply and demand, which brings the risk of cost increase to the economic dispatch. This paper mainly studies IES with energy hub as the research object, and studies the IES modeling and the optimal scheduling problem considering Conditional Value-at-Risk (CVaR). Firstly, the mathematical model of energy hub is established. Next, the network model of power system and natural gas system is established and the energy hub is reasonably connected to them. Then, for analyzing the uncertainty of wind power output, this paper develops scenarios using Latin hypercube sampling method and uses K-medoids clustering algorithm to reduce the scenarios. After defining the risk cost under uncertainty, CVaR is introduced into the objective function of IES optimal dispatch to describe the risk which operating personnel faces. Based on CVaR, the IES scheduling model is established and linearized into a mixed integer linear programming problem to be solved. Finally, numerical case studies verify that the IES scheduling model can reduce the risks with least costs and determine whether the system needs to avoid risks.

1. Introduction

In order to alleviate the problems of energy shortage and environmental pollution, the concept of integrated energy system (IES) is proposed, which involves regional electricity, gas and heat energy conversion, distribution and coordination. It is estimated that by 2030, gas power generation will increase by 230% [1], and the corresponding installed capacity of gas turbines will increase rapidly, further deepening the coupling degree within the IES [2]. As the degree of coupling continues to increase, its economy and reliability will affect each other. The traditional independent analysis method based on single energy system is no longer applicable. It is urgent to seek the coordinated optimization operation mode from the perspective of IES. Moreover, the concept of energy hub (EH) brings convenience to the analysis and modeling of IES. An energy hub is considered as a unit where multiple energy carriers can be converted, conditioned, and stored. It represents an interface between different energy infrastructures and loads [3].

At present, researches on IES can be roughly divided into several aspects: 1) IES modeling and energy flow analysis; 2) IES coordinated planning; 3) IES coordinated operation; 4) IES market coordination; 5) IES reliability analysis [4]. On the basis of analyzing the micro IES structure, the study in [5] takes advantage of the geographic resource, putting forward the regional IES economic optimization plan

Content from this work may be used under the terms of the Creative Commons Attribution 3.0 licence. Any further distribution of this work must maintain attribution to the author(s) and the title of the work, journal citation and DOI.
Published under licence by IOP Publishing Ltd

and control strategy to realize the optimal coordination of energy supply and demand. The study in [6] makes advance control of a fully integrated energy system for a building. However, it is worth noting that there are a large number of uncertainties in IES, such as the output of intermittent new energy. The study in [7] combines Monte-Carlo method and demand response technology to construct a random day-time optimization scheduling model of power-natural gas integrated community energy system (ICES) for increasing flexibility in the operation of ICES. The studies of [8-9] use multiple time-scale optimization and multi agent system based adaptive protection for integrated distribution systems, respectively. The existence of uncertainty will bring potential risks to the economic dispatch of the system. In the stochastic programming, there are many ways to deal with risks brought by uncertainty, such as variance method, expected loss, and ruin probability. As an effective risk assessment tool, Conditional Value-at-Risk (CVaR) has been applied in the field of optimization scheduling. The research in [10] transforms system security constraints into risk constraints, and extends CVaR to scheduling research as a technical breakthrough, but does not take into account the quantitative impact of the overall risk cost on the dispatcher.

In summary, the contribution of this paper is to further quantitatively evaluate the risk costs for the optimal scheduling of the IES, as well as to further analyze the severity of the scheduling risks caused by the uncertainty, providing the dispatcher a judgment whether or not avoiding the risks.

The rest of this paper is organized as follows. The methods of valuing risks are discussed in Section 2. And then, Section 3 presents the model formulation. In Section 4, the numerical examples verify the effectiveness and feasibility of the proposed method. Finally, Section 5 draws main conclusions in this paper.

2. Methods of valuing risks

In view of the uncertainty of wind power, the paper extracts samples by stochastic sampling, and then reduces the number of samples to the representative ones by scenario reduction method, so as to turn continuous uncertain samples into discrete deterministic samples and meet the demand of stochastic programming and CVaR.

In the field of scenario generation, Monte Carlo random sampling has been widely used, but Monte Carlo sampling has an inevitable shortcoming: in order to simulate the original distribution as much as possible, it needs enough samples. However, the principle of Latin hypercube sampling is different. It is based on the principle of stratified sampling. The sample is regarded as a cube, covering the various levels of the sample for representative sampling. So, it can be closer to the original sample distribution, and can replace most of the similar samples with fewer samples, which reduces the sample size and also reduces the number of samples.

The main principle of scenario reduction is to minimize the probability distance between the original scenario and the reduced scenario. This idea has something in common with the idea of the clustering algorithm. At present, the most popular clustering algorithms mainly include the K-means method and the K-medoids method. The K-means method clusters with the mean, which may change the characteristics of the original scenario. Therefore, this paper adopts the K-medoids clustering method in which the cluster center is the scenario, so as to avoid the loss of sensitivity to some extreme scenarios, and maintain the characteristics of the original scenario.

In order to improve the method of Value-at-Risk (VaR), Scholar Rockafeller and Uryasev published an improved method of valuing risks in 2002 [11]: Conditional Value-at-Risk (CVaR), which is used to specifically indicate how much average loss will be generated in a given investment time when the risk is more than the risk expectation under a given probability, which can be expressed by equation (1).

$$\mathrm{CVaR}_{\beta}(X) = E[f(X,\xi) \mid f(X,\xi) > \mathrm{VaR}_{\beta}] \tag{1}$$

Where, $f(X,\xi)$ for the loss function, ξ for the continuous random variable. The CVaR can not only evaluate the risk function of the normal distribution, but also evaluate the risk of any distribution function. In addition, its expectation value of the loss can effectively estimate the investment level when the adverse situation occurs. The discretization calculation is formulated by equation (2).

$$
\begin{aligned}
CVaR_{\beta} &= E[f(X,\xi) \mid f(X,\xi) > VaR_{\beta}] \\
&= VaR_{\beta} + E[f(X,\xi) - VaR_{\beta} \mid f(X,\xi) > VaR_{\beta}] \\
&= VaR_{\beta} + \sum_{n=1}^{N} \max\{f(X,\xi) - VaR_{\beta}\} \cdot \frac{P_{rn}}{P_r\{f(X,\xi) > VaR_{\beta}\}} \\
&= VaR_{\beta} + \frac{1}{1-\beta} \cdot \sum_{n=1}^{N} P_{rn} \cdot [f(X,\xi) - VaR_{\beta}]^{+}
\end{aligned}
\tag{2}
$$

Where, P_{rn} for the probability of scenario n. The calculation method obtained at this time still needs to calculate VaR first before calculating CVaR, which brings inconvenience to the calculation. Therefore, equation (3) is constructed. By solving this optimization, it is possible to simultaneously derive the objective function as CVaR and the auxiliary variable z as VaR.

$$
\min\ f(X,z) = z + \frac{1}{1-\beta} \cdot \sum_{n=1}^{N} P_{rn} \cdot [f(X,\xi) - z]^{+} \tag{3}
$$

3. Model Formulation

3.1. Objective function

$$
\min(C^{\text{base}} + C^{\text{risk}} + \beta \text{CVaR}) \tag{4}
$$

$$
C^{\text{base}} = \sum_{t=1}^{T}\left(C_t^{\text{s}} + C_t^{\text{sto}} + C_t^{\text{w}} + C_t^{\text{shed}}\right) + \sum_{t=1}^{T}\left(\sum_{g\in G} C_g P_{gt}^{\text{G}} + \sum_{s\in S} C_s P_{st}^{\text{Wcurtail}}\right) + \sum_{t=1}^{T}\left(\sum_{q\in Q} C_q F_{qt}^{\text{Q}}\right) \tag{5}
$$

$$
C^{\text{risk}} = \sum_{w\in\Omega} p(w)\left[\sum_{t\in T}\sum_{g\in G} C_g R_{gtw} + \sum_{t\in T}\sum_{s\in S} C_{sa}(P_{stw}^{\text{W}} - P_{st}^{\text{W}} - P_{stw}^{\text{Wcurtail}}) + \sum_{t\in T}\sum_{s\in S} C_{sw} P_{stw}^{\text{Wcurtail}}\right] \tag{6}
$$

$$
\text{CVaR} = \min_{\zeta,\eta_w} \zeta + \frac{1}{1-\alpha} \sum_{w\in\Omega} p(w)[C^{\text{base}} + C^{\text{risk}} - \zeta]^{+} \tag{7}
$$

In a scheduling period, the objective function consists of three parts. The first part is the normal cost of daily scheduling arrangement, the second part is the risk cost of the real-time operation, and the last part is the CVaR. It is worth noting that CVaR is multiplied by a risk factor, which is used to assess the degree of aversion of the dispatcher to the risk, as in equation (4). When β is equal to 0, CVaR does not exist, the system operates without considering the potential risk cost. When β is tiny, the system begins to avoid risk, and pursues small scheduling cost but faces greater risk of fluctuation. At this time, CVaR is large. When β is large, the system tries hard to avoid risks to make the risk of fluctuation under control with high scheduling cost. At this time, CVaR is small.
Where C^{base} is the total cost of energy hub operation, including the cost of purchasing electricity and gas C_t^{s}, the cost of energy storage equipment C_t^{sto}, the penalty of wind power curtailment C_t^{w} and the penalty for load shedding C_t^{shed}. Moreover, in equation (5), C^{base} also includes generator output cost, the curtailment penalty of wind farm and gas source cost.
Where C^{risk} is the risk cost, Ω is the scenario set, R_{gtw} represents the adjustment power of the generator, C_{sa} and C_{sw} represents the wind turbine adjustment maintenance cost and the curtailment penalty cost of the scenario w respectively, P_{stw}^{W} and $P_{stw}^{\text{Wcurtail}}$ respectively represents the actual output and the curtailment wind power in the scenario w.

Where ζ is the VaR to be optimized, α is confidence level, $p(w)$ is the probability of each scenario. Expression [x]+ equals max(x,0).

3.2. Constrains

3.2.1. Constrains of energy hub. It includes devices for storagement and conversion of power energy, gas and heat.

$$P_t^{\mathrm{s}} + P_t^{\mathrm{w}} + \sum_{i\in G^{\mathrm{CHP}}} P_{i,t}^{\mathrm{CHP}} + \sum_{i\in G^{\mathrm{b}}} P_{i,t}^{\mathrm{out}} = P_t^{\mathrm{d}} + \sum_{i\in G^{\mathrm{pump}}} P_{i,t}^{\mathrm{pump}} + \sum_{i\in G^{\mathrm{b}}} P_{i,t}^{\mathrm{in}} - P_t^{\mathrm{shed}} \quad \forall t \tag{8}$$

$$F_t^{\mathrm{s}} + \sum_{i\in G^{\mathrm{g}}} F_{i,t}^{\mathrm{out}} = F_t^{\mathrm{d}} + \sum_{i\in G^{\mathrm{CHP}}} F_{i,t}^{\mathrm{CHP}} + \sum_{i\in G^{\mathrm{boiler}}} F_{i,t}^{\mathrm{boiler}} + \sum_{i\in G^{\mathrm{g}}} F_{i,t}^{\mathrm{in}} - F_t^{\mathrm{shed}} \quad \forall t \tag{9}$$

$$\sum_{i\in G^{\mathrm{CHP}}} Q_{i,t}^{\mathrm{CHP}} + \sum_{i\in G^{\mathrm{boiler}}} Q_{i,t}^{\mathrm{boiler}} + \sum_{i\in G^{\mathrm{pump}}} Q_{i,t}^{\mathrm{pump}} + \sum_{i\in G^{\mathrm{h}}} Q_{i,t}^{\mathrm{out}} = Q_t^{\mathrm{d}} + \sum_{i\in G^{\mathrm{h}}} Q_{i,t}^{\mathrm{in}} - Q_t^{\mathrm{shed}} \quad \forall t \tag{10}$$

$$0 \le P_t^{\mathrm{s}} \le \bar{P}_t^{\mathrm{s}} \quad \forall t \tag{11}$$

$$0 \le F_t^{\mathrm{s}} \le \bar{F}_t^{\mathrm{s}} \quad \forall t \tag{12}$$

$$P_{i,t}^{\mathrm{CHP}} = \partial_i \eta_i^{\mathrm{e,CHP}} F_{i,t}^{\mathrm{CHP}} \quad \forall i, \forall t \tag{13}$$

$$Q_{i,t}^{\mathrm{CHP}} = (1\text{-}\partial_i) \eta_i^{\mathrm{h,CHP}} F_{i,t}^{\mathrm{CHP}} \quad \forall i, \forall t \tag{14}$$

$$0 \le P_{i,t}^{\mathrm{CHP}} \le \bar{P}_i^{\mathrm{CHP}} \quad \forall i, \forall t \tag{15}$$

$$-\Delta \underline{P}_i^{\mathrm{CHP}} \le P_{i,t+1}^{\mathrm{CHP}} - P_{i,t}^{\mathrm{CHP}} \le \Delta \bar{P}_i^{\mathrm{CHP}} \quad \forall i, \forall t \tag{16}$$

$$Q_{i,t}^{\mathrm{pump}} = \eta_i^{\mathrm{pump}} P_{i,t}^{\mathrm{pump}} \quad \forall i, \forall t \tag{17}$$

$$0 \le Q_{i,t}^{\mathrm{pump}} \le \bar{Q}_i^{\mathrm{pump}} \quad \forall i, \forall t \tag{18}$$

$$-\Delta \underline{Q}_i^{\mathrm{pump}} \le Q_{i,t+1}^{\mathrm{pump}} - Q_{i,t}^{\mathrm{pump}} \le \Delta \bar{Q}_i^{\mathrm{pump}} \quad \forall i, \forall t \tag{19}$$

$$Q_{i,t}^{\mathrm{boiler}} = \eta_i^{\mathrm{boiler}} F_{i,t}^{\mathrm{boiler}} \quad \forall i, \forall t \tag{20}$$

$$0 \le Q_{i,t}^{\mathrm{boiler}} \le \bar{Q}_i^{\mathrm{boiler}} \quad \forall i, \forall t \tag{21}$$

$$-\Delta \underline{Q}_i^{\mathrm{boiler}} \le Q_{i,t+1}^{\mathrm{boiler}} - Q_{i,t}^{\mathrm{boiler}} \le \Delta \bar{Q}_i^{\mathrm{boiler}} \quad \forall i, \forall t \tag{22}$$

$$E_{i,t+1}^{\mathrm{x}} = E_{i,t}^{\mathrm{x}} + X_{i,t}^{\mathrm{in}} \eta_i^{\mathrm{x,in}} \Delta t - \frac{X_{i,t}^{\mathrm{out}} \Delta t}{\eta_i^{\mathrm{x,out}}} \quad \forall i, \forall t \tag{23}$$

$$0 \le E_{i,t}^{\mathrm{x}} \le \bar{E}_i^{\mathrm{x}} \quad \forall i, \forall t \tag{24}$$

$$0 \le X_{i,t}^{\mathrm{in}} \le \beta_{i,t}^{\mathrm{x}} \bar{X}_i^{\mathrm{in}} \quad \forall i, \forall t \tag{25}$$

$$0 \le X_{i,t}^{\mathrm{out}} \le (1-\beta_{i,t}^{\mathrm{x}}) \bar{X}_i^{\mathrm{out}} \quad \forall i, \forall t \tag{26}$$

$$E_{i,T}^{\mathrm{x}} = E_{i,0}^{\mathrm{x}} \tag{27}$$

$$0 \le P_t^{\mathrm{w}} \le \bar{P}_t^{\mathrm{w}} \quad \forall t \tag{28}$$

$$P_t^{\mathrm{w,c}} = \bar{P}_t^{\mathrm{w}} - P_t^{\mathrm{w}} \quad \forall t \tag{29}$$

$$0 \le P_t^{\mathrm{shed}} \le P_t^{\mathrm{d}} \quad \forall t \tag{30}$$

$$0 \le F_t^{\mathrm{shed}} \le F_t^{\mathrm{d}} \quad \forall t \tag{31}$$

$$0 \le Q_t^{\mathrm{shed}} \le Q_t^{\mathrm{d}} \quad \forall t \tag{32}$$

Where equations (8)-(10) are supply and demand balance constraints. Equations (11)-(12) are purchase constraints. Equations (13)-(16) are combined heat and power (CHP) constraints. Equations (17)-(19) are pump constraints. Equations (20)-(22) are boiler constraints. Equations (23)-(27) are energy storage equipment constraints. Equations (28)-(29) are distributed power constraints. Equations (30)-(32) are load shedding constraints.

3.2.2. Constrains of network. It includes power system constrains and gas system constrains, which uses DC method of power flow calculation and piecewise linearization of nonlinear function, respectively.

$$\sum_{g\in\Phi_n^G} (P_{gt}^{\mathrm{G}} + R_{gtw}) + \sum_{g\in\Phi_n^S} (P_{stw}^{\mathrm{W}} - P_{stw}^{\mathrm{Wcurtail}}) - \sum_{m\in\psi_n} P_{nmtw}^{\mathrm{line}} - \sum_{d\in D} P_{dt}^{\mathrm{load}} = 0 \tag{33}$$

$$P_{nmtw}^{\mathrm{line}} = B_{nm} (\delta_{ntw} - \delta_{mtw}) \tag{34}$$

$$\sum_{s\in S} P_{st}^{\mathrm{W}} + \sum_{g\in G} P_{gt}^{\mathrm{G}} - \sum_{d\in D} P_{dt}^{\mathrm{load}} = \sum_{m\in\psi_n} AP_{nmt}^{\mathrm{line}} \quad \forall t \tag{35}$$

$$\underline{P}_{gt}^{\mathrm{G}} \le P_{gt}^{\mathrm{G}} + R_{gtw} \le \bar{P}_{gt}^{\mathrm{G}} \quad \forall t \tag{36}$$

$$-\Delta \underline{P}_{gt}^{\mathrm{G}} \le P_{g(t+1)}^{\mathrm{G}} + R_{g(t+1)w} - P_{gt}^{\mathrm{G}} - R_{gtw} \le \Delta \bar{P}_{gt}^{\mathrm{G}} \quad \forall t \tag{37}$$

$$\underline{P}_{nmt}^{\text{line}} \le P_{nmtw}^{\text{line}} \le \overline{P}_{nmt}^{\text{line}} \quad \forall t \tag{38}$$

$$\underline{\delta}_{nt} \le \delta_{ntw} \le \overline{\delta}_{nt} \quad \forall t \tag{39}$$

$$\sum_{q\in Q} F_{qt}^{\text{Q}} - \sum_{d\in D} F_{dt}^{\text{load}} = \sum_{i\in\psi_j} A_{gas} F_{gas,l}^{ij,t} \quad \forall t \tag{40}$$

$$S(i,j,t) F_{gas,l}^{ij,t\;2} = K_{ij}(p_{i,t}{}^2 - p_{j,t}{}^2) \tag{41}$$

$$S(i,j,t) = \begin{cases} 1, & p_{i,t} \ge p_{j,t} \\ -1, & p_{i,t} < p_{j,t} \end{cases} \tag{42}$$

$$\underline{F}_{qt}^{\text{Q}} \le F_{qt}^{\text{Q}} \le \overline{F}_{qt}^{\text{Q}} \quad \forall t \tag{43}$$

$$\underline{F}_{gas,l}^{ij,t} \le F_{gas,l}^{ij,t} \le \overline{F}_{gas,l}^{ij,t} \quad \forall t \tag{44}$$

$$\underline{p}_{i,t} \le p_{i,t} \le \overline{p}_{i,t} \quad \forall t \tag{45}$$

Where equations (33)-(35) are power flow constraints. Equations (36)-(37) are generator output upper and lower limits and climbing rate constraints. Equation (38) is line transmission power constraint. Equation (39) is voltage phase angle constraints. Equation (40) is natural gas balance. Equations (41)-(42) are Weymouth equation, which relates gas flow in gas pipeline and pressure of its two terminal nodes. The Weymouth equation can be linearized by the method in [12]. Equation (43) is gas source upper and lower limits. Equation (44) is line transmission flow constraint. Equation (45) is pressure constraint.

The proposed scheduling model is a mixed integer linear programming (MILP), which can be solved with the solvers, such as CPLEX, GUROBI. Due to space limitation of paper, the meaning of variables can be referred in [13].

4. Numerical Results

4.1. Case description

The proposed hardening strategy is examined on a test system consisted of IEEE 4-bus power distribution system, 4-node gas distribution system, one energy hub combining the two and one wind farm, as shown in figure 1.

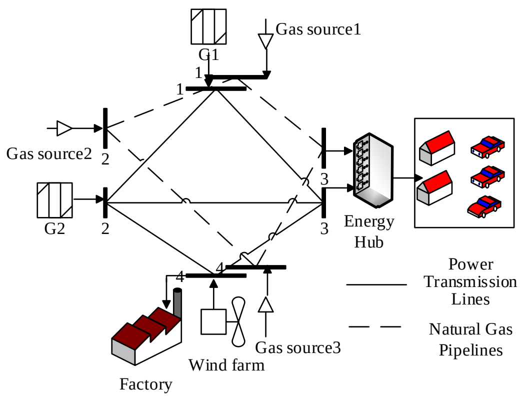

Figure 1. 4-node grid-4 node gas network diagram.

The parameters of devices of energy hub are:

CHP: ∂_1 =0.8, $\eta_1^{\text{e,CHP}}$ =0.4, $\eta_1^{\text{h,CHP}}$ =0.5, $\overline{P}_1^{\text{CHP}}$ =1.2MW, $\Delta\overline{P}_1^{\text{CHP}} = \Delta\underline{P}_1^{\text{CHP}}$ =0.5MW; pump: η_1^{pum} =0.6, η_2^{pum} =0.5, $\overline{Q}_1^{\text{pum}}$ =1.5MBtu, $\overline{Q}_2^{\text{pum}}$ =1MBtu, $\Delta\overline{Q}_1^{\text{pum}}$ = 0.6MBtu/h, $\Delta\overline{Q}_2^{\text{pum}}$ =0.5MBtu/h, $\Delta\underline{Q}_2^{\text{pum}} = \Delta\underline{Q}_2^{\text{pum}}$ =0.6 MBtu/h; boiler: η_1^{boi} =0.6, $\overline{Q}_1^{\text{boi}}$ =1.5MBtu, $\Delta\overline{Q}_i^{\text{boi}}$ = 0.5MBtu/h, $\Delta\underline{Q}_i^{\text{boi}}$ =0.4MBtu/h; battery: $\eta_1^{\text{bat,ch}}$ =0.8, $\eta_2^{\text{bat,ch}}$ =0.75, $\eta_1^{\text{bat,dch}}$ =0.8, $\eta_2^{\text{bat,dch}}$ =0.75, $\overline{E}_1^{\text{bat}}$ =5MW·h, $\underline{E}_1^{\text{bat}}$ =0.5 MW·h, $\overline{E}_2^{\text{bat}}$ =4MW·h, $\underline{E}_2^{\text{bat}}$ =0.4MW·h, $\overline{P}_1^{\text{ch}}$ =0.6MW, $\overline{P}_2^{\text{ch}}$ =0.5MW, $\overline{P}_1^{\text{dch}}$ =0.8MW, $\overline{P}_2^{\text{dch}}$ =0.75MW, gas storagement: $\eta_1^{\text{gs,ch}}$ =0.95, $\eta_1^{\text{gs,dch}}$ =0.95, $\overline{E}_1^{\text{gs}}$ =40kcf, $\underline{E}_1^{\text{gs}}$ =6kcf, $\overline{F}_1^{\text{ch}}$ =4kcf/h, $\overline{F}_1^{\text{dch}}$ =10kcf/h.

4.2. Case analysis

First of all, the supply of active power load, gas load and heat load are shown in figure 2.

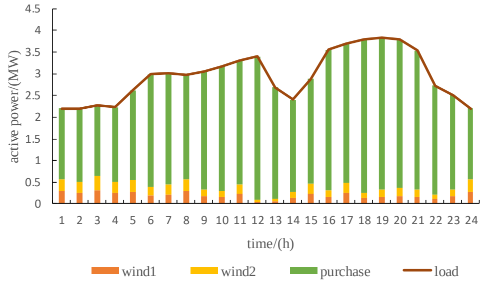

(a)

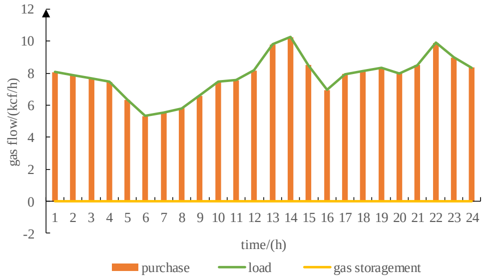

(b)

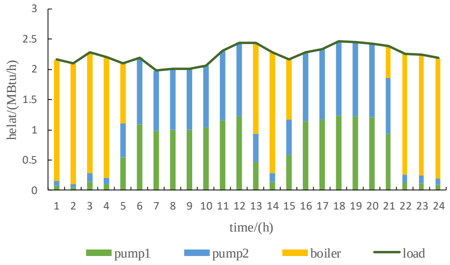

(c)

Figure 2. The supply of load. (a) active power load; (b) gas load; (c) heat load.

The values of risk coefficient are set to be 0, 0.2, 0.4, 0.8, 1, 2, and 3, respectively. Table 1 lists the values of the operation cost, risk cost, total dispatch cost, and CVaR under each risk coefficient. It can be seen that the total dispatch cost increases with the increase of the risk coefficient, and the CVaR decreases as the risk coefficient increases. Among them, the total dispatch cost increases from 21,233.44 euros to 21,258.12 euros, while the CVaR decreases from 21,321.68 euros to 21,293.59 euros. Based on the results of this table, figure 3 can be drawn showing the approximate effective cost boundary of the total dispatch cost with respect to the CVaR. It can be seen that when β is small, that is, the degree of aversion to risk is low, the dispatch cost increases slowly as the CVaR decreases. When β is large, that is, the risk aversion is at higher level, a lower level of CVaR value will result in a larger increase in total dispatch cost.

Table 1. Cost under each risk coefficient.

Risk coefficient β	Operation cost/€	Risk cost/€	Total dispatch cost/€	CVaR /€
0	21 149.09	84.36	21 233.44	\
0.2	21 149.33	84.36	21 233.68	21 315.68
0.4	21 146.22	88.33	21 234.55	21 312.58
0.8	21 140.18	99.38	21 239.56	21 306.54
1	21 138.20	102.40	21 240.61	21 304.56
2	21 153.02	99.51	21 252.53	21 296.27
3	21 159.15	98.97	21 258.12	21 293.59

Two scheduling schemes with different typical β are compared in figure 4. When the risk is avoided, the maximum generator adjustment amount is reduced by nearly half from 7 to 3, and the abandoned wind power is higher than or equal to the non-avoidance risk situation. When taking risks, the system is more inclined to abandon the wind and reduce the amount of generator adjustment to achieve the purpose of no load shedding.

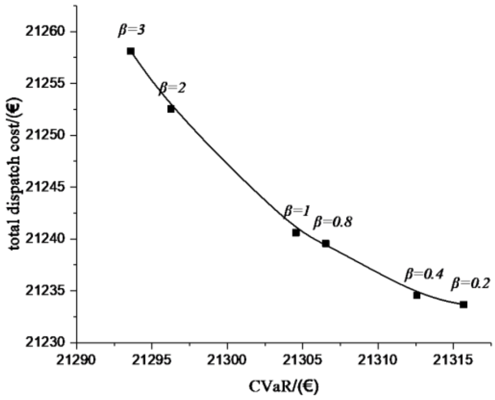

Figure 3. Effective boundary between total dispatch cost and CVaR.

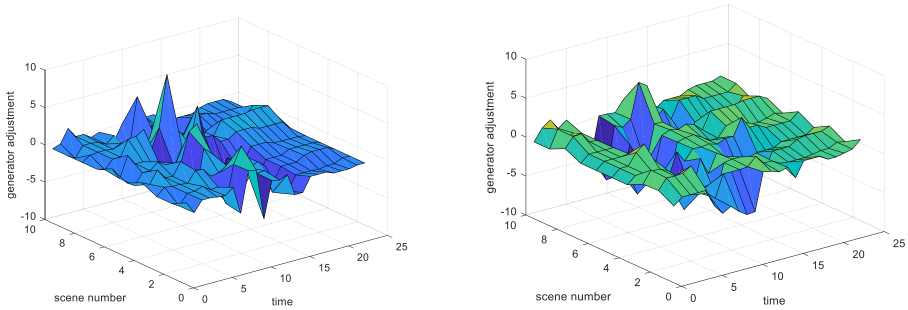

(a) β =0 (b) β =1

Figure 4. Generator adjustment comparison.

It can be seen from figure 3 that there is a contradiction between economics and risk avoidance. In order to obtain a cost-effective risk coefficient value, with which the increase of unit dispatch cost can maximize the reduction of CVaR, this paper introduces the concept of "marginal" in economics and defines a marginal cost of CVaR, called as the marginal risk cost. It can be defined as the ratio of the CVaR growth to the cost growth, as in equation (46):

$$\mathrm{MC(CVaR)} = \frac{\Delta \mathrm{CVaR}}{\Delta \mathrm{TC}} \tag{46}$$

Where $\mathrm{MC(CVaR)}$ is the marginal risk cost. $\Delta\mathrm{CVaR}$ is change amount of CVaR and $\Delta\mathrm{TC}$ is change amount of total cost. By data processing, a curve of marginal risk cost can be drawn as shown in figure 5.

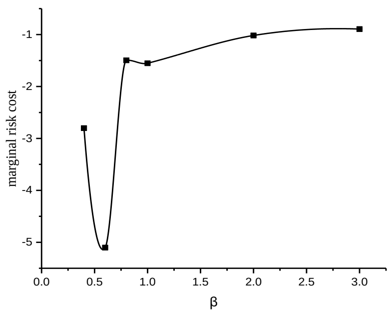

Figure 5. Marginal risk cost of CVaR.

 1585 (2020) 012043 doi:10.1088/1742-6596/1585/1/012043

The greater the absolute value of marginal risk cost is, the more efficient the reduction of CVAR can be achieved, making our investment more cost-effective and achieve a balance between economy and risk. In this test system, the lowest point of the curve is the cost-effective optimal value of β, at which $\beta = 0.6$.
To further verify the correctness and applicability of the model proposed, a more complex system is calculated. The example keeps the uncertainty of wind power output the same, and changes the 4-node grid for the IEEE 30-node grid as shown in figure 6.

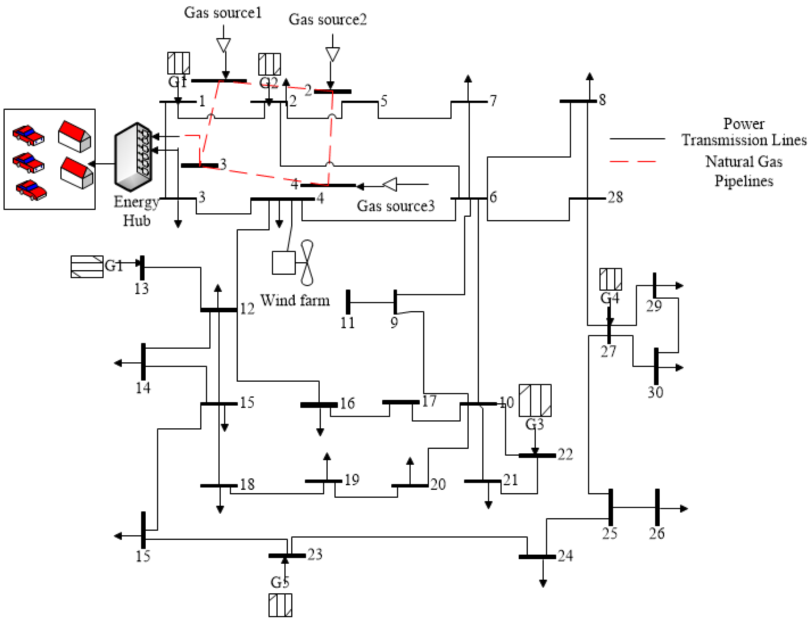

Figure 6. IEEE 30-node grid-4 node gas network diagram.

By analyzing in the similar way, it is clear to find from figure 7 that the effectiveness boundary shows a consistent curve trend. It verifies the applicability of the model. However, the marginal risk cost is different from the previous system, because the same scale of the wind power is much smaller for the current system scale. Therefore, there is no need to avoid risk and a smaller β is enough.

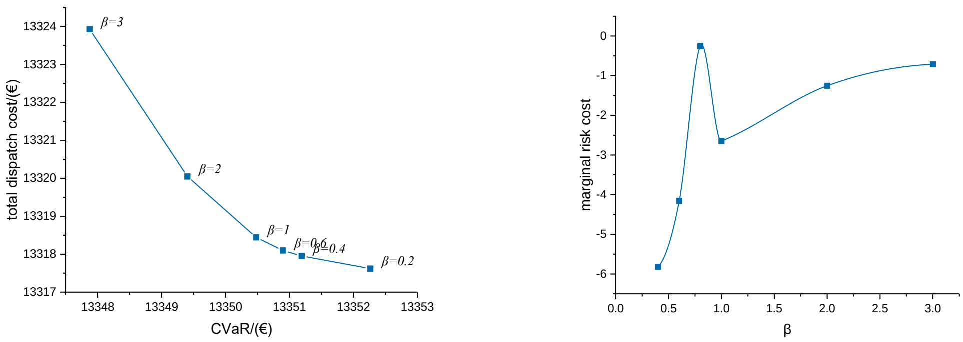

(a) (b)

Figure 7. IEEE 30-node grid-4 node gas network: (a) effective boundary (b) marginal risk cost.

5. Conclusions

This paper establishes an optimal dispatch model for integrated energy systems that takes into account the CVaR. The model can determine the dispatch output of the supply side and the operation mode of the EH within 24 hours with the minimum costs and CVaR under the condition of satisfying the balance of energy supply and demand. CVaR is used to describe the risk which operating personnel faces due to the uncertainty of wind power output. By introducing CVaR into the objective function of IES optimal dispatch, operators can determine confidence levels based on their level of risk aversion. By introducing marginal risk cost into the analysis, operators can obtain a cost-efficient risk coefficient so that they can reduce the risks they may face with least costs. The numerical examples verify the effectiveness and feasibility of the proposed method.

6. References

[1] Correa-Posada CM and SáNchez-Martın P 2014 *IEEE Transactions on Power Systems* **29** 1780-1787
[2] Liu C , Shahidehpour M and Wang J 2010 *IET Generation Transmission & Distribution* **4** 1314-1325
[3] Geidl M, Koeppel G and Favre-Perrod P 2015 *IEEE Power and Energy Magazine* **5** 24- 30
[4] Chen S, Wei Z and Sun GQ 2015 *Proceedings of the CSEE* **35** 6331-6340
[5] Yu HB, Zhang C and Deng ZQ 2018 *Mordern Power Systems and Clean Energy* **6** 330-341
[6] J. M. Counsell, Al Khaykan Ameer , M. J. Stewart 2016 *IEEE Transactions on Power Systems* **4** 1314-1325
[7] Zhang XP, Shahidehpou RM, Alabdulwahab A 2016 *International Journal of Smart Grid and Clean Energy* **5** 229-236
[8] Yajie Huanga, Junyong Wua, Xingyan Niub, Shiqiao Gaob 2019 *International Journal of Smart Grid and Clean Energy* **8** 263-270
[9] Chengxi Liua*, Zakir Hussain Rathera,b, Zhe Chena, Claus Leth Baka 2013 *International Journal of Smart Grid and Clean Energy* **2** 406-412
[10] Zhou RJ, Yao LH, Tong XJ 2012 *Proceedings of the CSEE* **32** 56-63
[11] Rockafellar RT, Uryasev S 2002 *Journal of Banking and Finance* **26** 1443-1471
[12] He C, Wu L, Liu TQ 2017 *IEEE Transactions on Sustainable Energy* **8** 658-670
[13] Qi SX, Wang XL, Li X 2019 *Sustainability* **11** 4048

Acknowledgments

This work is supported in part by Science and Technology Foundation of SGCC (Research on Morphologies and Pathways of Future Power System).